J. Fluid Mech. (1974), *vol.* 62, *part* 2, *pp.* 273–287
Printed in Great Britain

Two-dimensional turbulence near the viscous limit

By J. S. A. GREEN
Department of Meteorology, Imperial College, London

(Received 8 May 1972 and in revised form 21 September 1973)

Two-dimensional incompressible motion is generated by a steady external body force varying sinusoidally with a transverse co-ordinate. Such flow is found to be unstable for Reynolds numbers greater than $2\frac{1}{2}$, and under these conditions evolves towards a new steady state. This 'steady-eddy' state is itself unstable in a sense, and its breakdown suggests the catastrophic onset of a cascade of turbulence. The mechanics of this cascade can be represented by a kind of recursion system in which the turbulence dynamics of one scale is repeated in the next, and a law of turbulent stress results. The spectrum of kinetic energy generated by a steady input of momentum at a discrete wavelength shows a rapid decrease (as k^{-5}) towards shorter wavelengths but a much slower decrease (as k) towards longer wavelengths.

1. Introduction

One of the fundamental problems in the theory of turbulence is that of relating the spectrum of the fully developed turbulent motion to the spectrum of the energy input. Here we tackle the simplest of these problems: given that energy enters the system at a single wavelength to deduce how this energy is redistributed by the consequent motion, assumed two-dimensional. Because this consequent motion is not uniquely defined (i.e. we *are* treating turbulence) additional hypotheses are needed in order to close the problem. These will be specified in physical, rather than ensemble, space, and this allows the conjectured evolution of the flow to be visualized rather readily.

We shall make the hypothesis that a theory relating the structure of *small* amplitude disturbances to the form of the laminar flow on which they are superposed can be used to infer some properties of the fully developed turbulent motion. This hypothesis has already proved useful in the description of the transfer properties of the large-scale baroclinic eddies of the troposphere (Green 1970) as regards their scale, intensity and fluxes of energy and of momentum. Here we shall suppose that the turbulence developed from a disturbance of infinitesimal amplitude initially superimposed on the mean flow. The final turbulent state reached is found to depend little upon the character of the initial disturbance.

The assumed two-dimensionality means that, for realistic truncations, algebraic manipulations are kept to a minimum but that direct comparison with those real flows that are essentially three-dimensional is unlikely to be profitable. In view of the speculative nature of the theory it is desirable that some

comparison be made with two-dimensional flows before embarking on a three-dimensional version.

While this paper was being reviewed my attention was drawn to a similar study by Lorenz (1972*b*). The treatments are, however, essentially different mainly because, though each relies on being able to separate out a small subset of important turbulent interactions in wavenumber space, the criteria for importance, and hence the interactions selected, are different.

2. The model system

Consider the motion generated by the body force **F** defined by the momentum equation

$$\rho\, D\mathbf{v}/Dt + \nabla p - \rho\nu\nabla^2\mathbf{v} = \mathbf{F},$$

where the flow is incompressible and buoyancy forces are neglected. The body force is to be thought of as the forcing due to sources of momentum not included explicitly. For example, in conditions of ordinary convection, buoyancy forces act as a source of vertical momentum and would be represented in **F**.

Again, large-scale quasi-horizontal baroclinic eddies in the atmosphere and oceans, because they tend to transfer conserved quantities (principally potential vorticity and energy) down-gradient, are thereby constrained to transfer momentum up-gradient and hence inject momentum into the baroclinic zones (see Green 1970). In this case the Reynolds stress behaves like a source of momentum for the mean flow. Where the resulting jets are unstable to barotropic disturbances (likely at least in the mesosphere, i.e. the layer of smaller static stability between about 60 and 80 km, and in the western boundary currents of the oceans) the present theory may be appropriate to the barotropic breakdown phase of the motion.

In order to have a well-defined scale of energy input we suppose that the body force varies sinusoidally in a transverse direction and is independent of time. Let the x axis be directed along the body force in the direction denoted by the unit vector **i** with the y axis in the perpendicular direction **j** and the body force have amplitude $\rho\chi$ and wavelength $2\pi/\mu$ in the y direction. A possible solution is the steady laminar flow given by

$$\left.\begin{aligned} v_x &= -(\chi/\mu^2\nu)\cos\mu y, \quad v_y = 0, \\ F_x &= -\rho\chi\cos\mu y, \quad F_y = 0 \end{aligned}\right\} \tag{1}$$

where

and ν is the kinematic coefficient of viscosity. This flow satisfies Rayleigh's criterion for inviscid instability and, as we shall show, a range of perturbations can grow with time.

We suppose that the eddy which grows most rapidly when of small amplitude will eventually dominate the finite amplitude flow. This hypothesis will be referred to below as the *selection principle*, and it implies that the flow remains two-dimensional. Thus Lin (1955, p. 27), reporting Squire, shows that any three-dimensional disturbance of a two-dimensional parallel flow will have the stability characteristics of an equivalent two-dimensional disturbance for a lower Reynolds number, so that the fastest growing eddy will be two-

dimensional and in the x, y plane. Assuming the fluid to be incompressible, a stream function ψ can be used for the velocity field,

$$v_x = -\partial\psi/\partial y, \quad v_y = \partial\psi/\partial x,$$

and the normal component of the vorticity equation usefully describes the flow:

$$\frac{D\zeta}{Dt} - \nu\nabla^2\zeta = -\frac{1}{\rho}\frac{\partial F_x}{\partial y}, \quad \text{where} \quad \zeta = \frac{\partial^2\psi}{\partial x^2} + \frac{\partial^2\psi}{\partial y^2}. \tag{2}$$

3. Linearized stability analysis of sinusoidally sheared flow

In the usual manner consider constant-shape perturbations of the initial flow defined by (1), with the stream function for the perturbation of the form

$$\psi' = \mathrm{Re}\{\exp(i\lambda x + \omega t) f(y)\},$$

where $2\pi/\lambda$ is the x wavelength and ω is the amplification rate of the perturbation. The condition that ψ' satisfies the linearized form of (2) can be written as

$$(\sigma - ip\cos\eta)\left(\frac{d^2f}{d\eta^2} - p^2 f\right) - ip(\cos\eta) f = \frac{1}{R}\left(\frac{d^2}{d\eta^2} - p^2\right)^2 f, \tag{3}$$

where $R = \chi/\nu^2\mu^3$ is a Reynolds number for the equilibrium flow, $\sigma = (\nu\mu/\chi)\omega$ is the non-dimensionalized amplification rate, $p = \lambda/\mu$ is the non-dimensionalized x wavenumber and $\eta = \mu y$ is the non-dimensionalized y co-ordinate. The solutions of (3) are not in general periodic in y, but in view of the periodicity in the mean flow and the absence of material boundaries it seems intuitively reasonable that the most unstable mode should be periodic in y and have the same wavelength as the original flow. If this assumption is made f can be expanded in the form

$$f = \sum_{n=-\infty}^{\infty} \frac{b_n e^{in\eta}}{n^2 + p^2 - 1}$$

and (3) is satisfied provided that the coefficients satisfy the three-point recurrence relation

$$b_{n+1} + b_{n-1} + \frac{2i}{p}\left(\frac{n^2+p^2}{n^2+p^2-1}\right)\left(\frac{n^2+p^2}{R} + \sigma\right) b_n = 0$$

(similar to that for Mathieu's equation). Dividing through by b_n we see that the ratio of successive coefficients is, for large n, either $b_{n+1}/b_n \sim -2in^2/pR$ or $ipR/2n^2$. The first series is divergent so is rejected. The second series gives two possible solutions: one odd, one even. The nature of the asymmetry of the odd solution (that with $b_0 = 0$) with respect to the mean flow field means that momentum cannot be transferred so as to decrease the kinetic energy of the original flow, hence that this solution must be stable (there is no alternative energy source). The even series (with $b_0 = 1$ say) is readily summed to any desired degree of accuracy and determines the eigenvalue ω (or σ) in terms of λ (or p). Taking only the first two terms of the series by putting $b_2 = b_{-2} = 0$ gives

$$\psi' = \cos\lambda x + \frac{2}{p}\left(\sigma + \frac{p^2}{R}\right)\sin\lambda x\cos\mu y$$

and

$$\sigma = -\left(\frac{1+2p^2}{2R}\right) + \left(\frac{1}{4R^2} + \frac{p^2(1-p^2)}{2(1+p^2)}\right)^{\frac{1}{2}}. \tag{4}$$

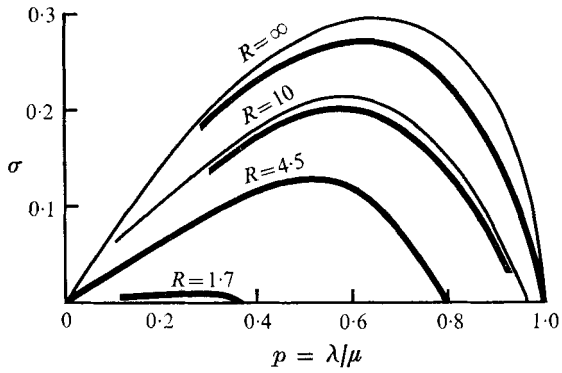

FIGURE 1. Growth rate σ of eddies in sinusoidally sheared flow as a function of wavenumber for different values of the Reynolds number $R = A/\nu$, where A is the amplitude of the stream function for the mean flow. Thin lines show the two-term approximation obtained from (4). Thick lines show accurate solutions obtained by summing more terms in the recurrence relation. Notice the well-defined maximum in the growth rate and the tendency for viscous dissipation to favour the longer waves.

This approximation is compared with accurate solutions (for which up to six terms need to be included) in figure 1, where it is seen to give a tolerable approximation. Even in the least favourable circumstance, where $R \to \infty$ and energy penetrates furthest towards short wavelengths, the two-term approximation to the amplification rate is correct to within 10 %. This fidelity is important because a similar two-term approximation forms the basis for the subsequent nonlinear calculations.

The flow satisfies Rayleigh's criterion for inviscid instability, and growing waves are possible for all values of the Reynolds number greater than $2\frac{1}{2}$. This is obviously true of the two-term approximation giving (4), and the following argument shows it to be true of the accurate solution. We seek the neutral wave (for which the amplification rate vanishes). Putting $\sigma = 0$ and letting $p^2 \to 0$ we find that the terms b_n contain, for $n \geqslant 2$, a contribution proportional to $(2 - R^2)/p^2$. Thus these higher coefficients become unbounded unless $R^2 \to 2$ as $p^2 \to 0$ for the neutral-stability curve.

Figure 1 shows that p is less than unity for growing eddies: that is, the (x) wavelength of the developing eddy is greater than the (y) wavelength of the original flow. Thus, as energy is transferred from the wavenumber μ of the basic flow to the higher wavenumber $(\lambda^2 + \mu^2)^{\frac{1}{2}}$ by the instability, energy also appears at the lower wavenumber λ. Some rather important consequences of this feature are discussed in §8. This property was demonstrated for two-dimensional, neutrally buoyant, *inviscid* flow by Fjørtoft (1953), who pointed out that, in that case, the total mean-square velocity and the total mean-square vorticity are each conserved: i.e. $\overline{(\nabla\psi)^2}$ and $\overline{(\nabla^2\psi)^2}$ are both constant, so that a transfer of kinetic energy to shorter wavelengths must be accompanied by a (greater) transfer to longer wavelengths.

Not unexpectedly, viscosity acts to diminish the amplification rate for all waves, particularly the shorter ones, so that for initial flows with smaller Rey-

nolds number the fastest growing wave is longer. Indeed, for $R^2 \to 2$ only the infinitely long wave can grow, and that infinitely slowly.

The detailed calculations show that the amplifying eddies are oriented such that they tend to smooth the initial field of momentum, consistent with their reducing the initial mean kinetic energy, which is thereby made available for eddy kinetic energy and viscous dissipation. The *inviscid* stability problem is identical with that recently treated by Lorenz (1972*a*).

4. The developing motion

In order to follow the solutions of the fully nonlinear equations to large amplitudes it is necessary to represent the solutions in finite terms, and here it is convenient to do this by truncating the Fourier series for the stream function. The first-order perturbation solution truncated to two terms in the y direction suggests one way in which such an expansion might be generated. Substituting

$$\psi = A \sin \mu y + B \cos \lambda x + D \sin \lambda x \cos \mu y \tag{5}$$

into the vorticity equation (2) gives terms in $\sin \mu y$, $\cos \lambda x$, $\cos \mu y \sin \lambda x$, $\sin \mu y \times \cos 2\lambda x$ and $\cos 2\mu y \cos \lambda x$ whose coefficients are listed as A_1, A_2, A_3, A_4 and A_7 in the appendix with $E = G = H = 0$. Of these terms the first, second and third are of the lowest spatial frequency but can be made to vanish if the coefficients A, B and D satisfy three nonlinear ordinary differential equations ($A_1, A_2, A_3 = 0$ from the appendix with $E = G = H = 0$). The terms A_4 and A_7, both of higher spatial frequency, cannot be eliminated and must remain as residual error in this truncation.

A useful test of the error due to this approximation comes from solving the linearized stability problem for the truncated system. Because of the way the truncation has been chosen this reproduces (4), which, as shown by figure 1, is indeed a fairly good approximation. The ψ field similarly truncated is found to be accurate to about 5 %.

5. Asymptotic steady state for simplest truncation

The three simultaneous equations $A_1, A_2, A_3 = 0$ can be integrated (at least numerically) with respect to time to find a first approximation to the evolving flow. However, we are most interested in the final state of the motion. This can be found without going through the intermediate steps because the truncated solution eventually settles down to a new steady state, which we shall call a 'steady-eddy flow'.

Some more precise numerical and analytic considerations of this evolution are reported later in this section and in § 6, but first we shall show that the steady-eddy flow is indeed well defined. Making this assumption, hence putting $d/dt = 0$ (and still $E = G = H = 0$) in the equations $A_1, A_2, A_3 = 0$, gives solutions of two types:

$$A = \chi/\nu\mu^3, \quad B = D = 0,$$

the laminar, equilibrium flow, or

$$A^2 = 2\nu^2 \frac{(1+p^2)^2}{1-p^2}, \quad D^2 = 4\nu^2 \left(\frac{\nu R}{A} - 1\right), \quad B = \frac{AD}{2\nu p}, \tag{6}$$

representing the steady-eddy motion. For the coefficient A to be real, p^2 must be less than unity. But if the pattern is the finite amplitude form of a growing eddy, § 3 and the selection principle together show this to be true, for the numerical value of p^2 is uniquely determined as a function of R by the maxima in figure 1, and is necessarily less than unity. The coefficient A must be positive for D to be real; so A is uniquely determined. The signs of B and D must be the same but may be positive or negative. This amounts to a change in x phase of π/λ, but this phase merely defines the point along the initially uniform flow at which the eddy will grow so is physically indeterminate anyway. Thus, if the final motion is steady and defined, via the selection principle, by the initial conditions, it can be found from (6). Notice that this final steady state represents the finite amplitude form of an eddy which grew in the initial flow, and is not the same as the 'critical waves' of infinitesimal amplitude which just fail to grow, given by $\sigma = 0$.

The amplitude of the new x-mean flow, given by A in (6) and shown as the thin curved line $3P$ in figure 2, is decreased compared with the laminar flow for the same forcing (the straight line in figure 2) because the transfer of momentum by the eddies is down-gradient and therefore adds to that due to viscosity.

It is of interest to inquire whether this steady-eddy flow is stable, in the sense that all small deviations of A, B and D from their steady-eddy values decrease with time. If such deviations are assumed to be proportional to $\exp(q\nu\mu^2 t)$ a little manipulation shows that the non-dimensional growth rate q satisfies

$$q(q+1)(q+1+2p^2) + (D^2/4\nu^2)\{(1+2p^2)q + 2p^2(1+p^2)\} = 0.$$

Stability is least likely when $D^2 \gg \nu^2$, for which case

$$q = -\frac{2p^2(1+p^2)}{1+2p^2} \quad \text{or} \quad \pm i\frac{(1+2p^2)^{\frac{1}{2}}}{2}\frac{D}{\nu} - \frac{(1+p^2)^2}{1+2p^2} + O\left(\frac{\nu}{D}\right).$$

The real part of all three roots being negative, all deviations from the steady-eddy state must decrease exponentially with time, showing that, in this sense, the steady eddy is a stable state. Results of a numerical test, reported in § 6 and shown in figure 3, are at least qualitatively in agreement with this result. Lorenz's similar three-term analysis of convective motion (1963) also shows stability in the appropriate limit $\kappa \gg \nu$.

6. More accurate solutions for the final steady state

The truncation errors have become considerable by $R = 5$, and more accurate solutions are desirable. These can be obtained by adding Fourier coefficients to the expansion of ψ and eliminating more of the lower order residuals. In this way the complete set of functions generated from the initial perturbation could, in principle, be obtained.

There are only two residuals in the three-parameter approximation, given by the terms A_4 and A_7 in the appendix, with $E = G = H = 0$. The coefficient of

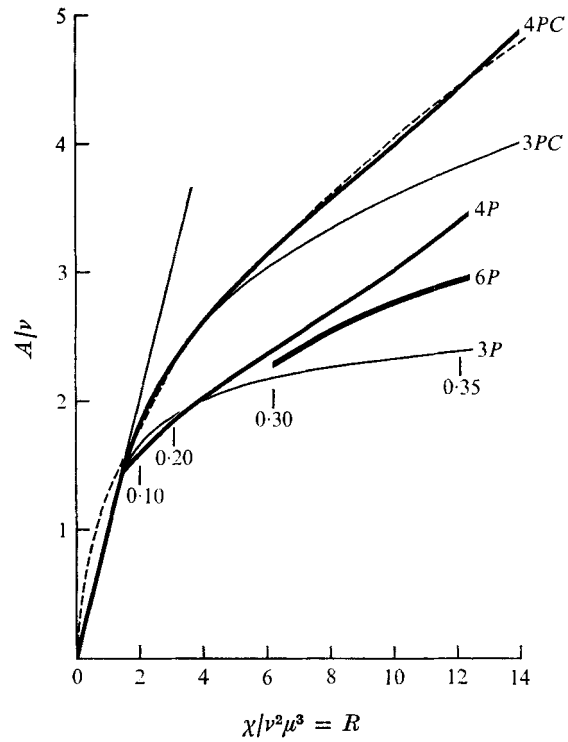

FIGURE 2. Amplitude A of mean flow as a function of the amplitude χ of the external forcing. The thin straight line shows the undisturbed steady, viscous, laminar solution. Curves $3P$, $4P$ and $6P$ show steady viscous eddy solutions with three, four and six parameters respectively; each solution uses the values of p^2 marked along the curves, which are consistent with the flow first attaining its steady laminar state then realizing its instability at the wavelength of maximum amplification rate. Curves $3PC$ and $4PC$ show cascade eddy solutions with three and four parameters respectively: in the cascade set the value of p^2 is that for the maximum amplification rate of a dominant small amplitude instability of the *final* mean flow. The dashed line shows values deduced from the 'turbulence' law (11).

$\cos\lambda x \cos 2\mu y$ is found to be small compared with the coefficient of $\cos 2\lambda x \sin \mu y$, and in the next approximation the latter is eliminated by adding the term

$$E \cos 2\lambda x \sin \mu y$$

to ψ given by (5). This results in residuals of higher order, containing products involving E, being introduced, like A_5 and A_6 in the appendix with $G = H = 0$, but the residuals are not all listed. The four simultaneous equations so defined, $A_1, \ldots, A_4 = 0$ from the appendix, with $G = H = 0$, again admit an analytic solution in closed form and all solutions can be found explicitly. Thus, putting $A = \nu R\alpha$ and using the equations $A_1, \ldots, A_4 = 0$ to eliminate the coefficients D and E then eliminating B, we find the laminar solution $\alpha = 1$, or the steady-eddy solution

$$\left(\alpha - \frac{(1+3p^2)(1-\alpha)}{2(1+4p^2)^2(1-p^2)}\right)\left(\alpha + \frac{3(1-\alpha)}{2(1+4p^2)^2}\right) = \frac{2(1+p^2)^2}{(1+p^2)R^2},$$

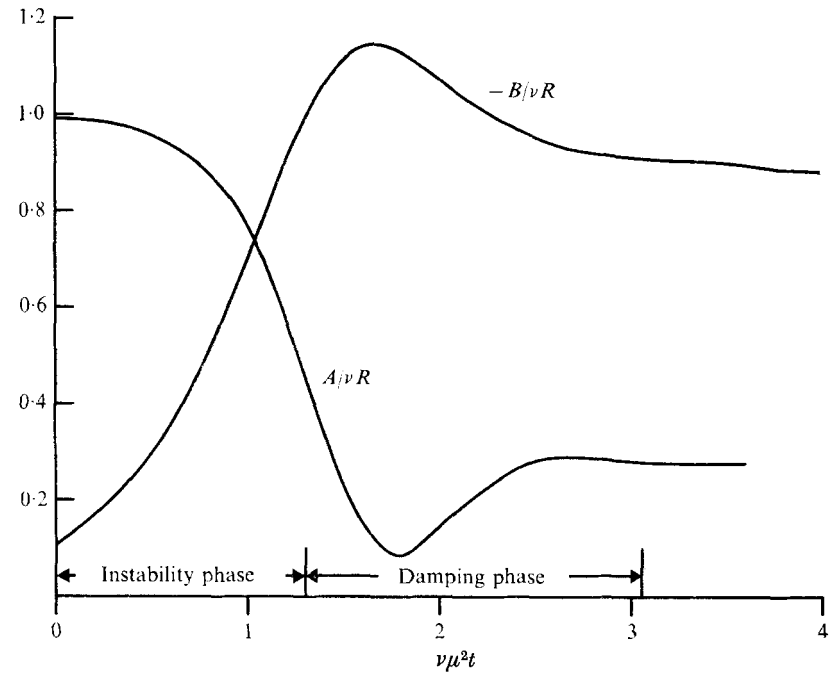

FIGURE 3. Coefficients $A/\nu R$ and $B/\nu R$ as a function of time, showing the behaviour of the mean flow and first eddy mode as the flow collapses. Notice the two distinct phases of evolution: the breakdown phase up to $\nu\mu^2 t \sim 1$ and the settling-down phase $1 < \nu\mu^2 t < 3$, also the final dominance of the eddy mode over the mean flow. The results are from a numerical solution to the six-parameter system with $R = 10$, $p^2 = 0{\cdot}4$; this is not in fact the wavenumber of maximum amplification rate as is evident from figure 1, but its behaviour is similar.

where p is the function of R determined through figure 1 by appeal to the selection principle. Of the two roots for α, one gives B imaginary so is rejected. The other gives B and D of the same undetermined sign, but as with the three-parameter solutions this corresponds only to an ambiguity in the (x) phase of the eddy, which is unimportant so far as its structure is concerned. Thus again we can show that the condition that the final state should be steady defines the flow unambiguously. Figure 2 shows, by a thicker line $4P$, values of A using this approximation and differing from the simplest approximation for $R > 5$ or so.

The largest residuals in the four-parameter approximation can be eliminated by adding the further terms

$$G\cos 3\mu y + H\cos\lambda x\sin 3\mu y$$

to ψ, giving the equations $A_1, \ldots, A_6 = 0$, obtained from the appendix (but without any of the residual terms). Analytic solutions could not be found, so numerical techniques were required. Even the numerical solution of such highly nonlinear simultaneous equations is by no means straightforward, so it was decided to integrate the time-dependent equations numerically with respect to time, starting from the solutions of small amplitude and proceeding until the final steady state was reached. This tests the previous assumption: that the solutions do indeed finally attain the asymptotic steady state.

In addition we get a picture of the temporal evolution as in figure 3, which shows an example of the variation with time of the two principal components of the flow. Evidently this evolution can be split into two separate phases, an instability phase in which the initial mean flow is eliminated mainly in favour of the B term, followed by a viscous phase in which the steady state is approached asymptotically. A number of such calculations were carried through and these show that the same final, steady state is reached from a variety of initial values of the coefficients (provided that χ and p^2 are unchanged), showing that there is temporal convergence of the finite amplitude motion using six parameters, as demonstrated in §5 for infinitesimal disturbances of the three-parameter solution.

Starting from a small but finite perturbation of laminar flow, the time t_* required to attain a steady state is given approximately by

$$t_* = \frac{1}{\nu\mu^2}\left(\frac{8}{R}+2\right)$$

for values of R between 10 and 50: a time scale for the unstable collapse of the initial flow plus a time scale for viscous damping to the final steady state. For this range of Reynolds numbers the viscous damping phase takes longer, though most of the change in the mean flow takes place during the instability phase. Values of A for the final steady-eddy state are given by the thick curve $6P$ in figure 2.

7. Convergence of successive solutions

The successive approximations to ψ given by the three-, four- and six-parameter solutions correspond to truncation with respect to the total wavenumber

$$k = (n^2\lambda^2 + m^2\mu^2)^{\frac{1}{2}}$$

for the relevant range $p^2 \leqslant 0{\cdot}375$ appropriate to the range $R < 50$, except that the term in $\cos 2\lambda x \cos \mu y$, whose residual is very small, has been ignored. Physical considerations lead one to suspect that a sequence of truncations in wavenumber space will converge because the action of viscosity is likely to limit the spread of energy into the higher wavenumbers. However, because of the unusual form of the equations for the steady-state coefficients it is difficult to interpret the consequences of given values of the residuals at any stage, other than in terms of the apparent consistency of the successive curves $3P$, $4P$ and $6P$ of figure 2, which is some evidence for convergence. Moreover, the dominance of B over A in the final stage ensures a fairly systematic decrease of amplitude with wavenumber (recall that B has the smallest k). This is illustrated by the crosses in figure 5, which are derived from the $6P$-solution for $R = 6$, which is typical.

The successive solutions appear to converge, at least asymptotically, in the limit of small instability where $p^2 \to 0$ and

$$R = 2^{\frac{1}{2}}\{1+3p^2+O(p^4)\}, \quad A = \nu 2^{\frac{1}{2}}\{1+O(p^4)\},$$
$$B = \nu 6^{\frac{1}{2}}\{1+\tfrac{9}{2}p^2+O(p^4)\}, \quad D = \nu\{2\times 3^{\frac{1}{2}}p+O(p^3)\}, \quad E = \nu\{3\times 2^{\frac{1}{2}}p^2+O(p^4)\},$$
$$G = \nu\{-\tfrac{2}{3}\times 6^{\frac{1}{2}}p^2+O(p^4)\}, \quad H = \nu\{3^{\frac{1}{2}}p^3+O(p^5)\}.$$

It is at first sight surprising that, as shown by this limiting case, the coefficient B should be discontinuous at the value ($R^2 = 2$, $p^2 = 0$) for critical stability, for B vanishes for $R^2 < 2$. However, the contribution to the velocity represented by pB is continuous, as is the kinetic energy, so all relevant physical variables are continuous.

The solutions have one disturbing property, which arises because of their steady nature. The eddy wavelength has been supposed determined at the time when the eddies were small perturbations on the viscous-equilibrium flow. In that respect the flow 'remembers' for ever its antecedents. An alternative, more plasusible, hypothesis might be that the dominant eddy is that which would grow fastest in the *existing* mean shear. This means that instead of finding the selected wavelength by using the Reynolds number for the equilibrium flow ($R = \chi/\nu^2\mu^3$) we should use a Reynolds number for the final mean flow, $R_m = A/\nu$. The plausibility of this hypothesis, related as it is to an important selection principle, would repay being tested in a numerical experiment of much greater resolution.

Curves $3P$, $4P$ and $6P$ in figure 2 are changed a little when this refined selection principle is used, and a region of intermittency appears for $\chi/\nu^2\mu^3$ less than 3 or so, but the overall correction is not as large as that arising in the next section, and so we defer its application until then.

8. The catastrophe and consequent cascade

In the steady-eddy flow, most of the kinetic energy appears in the first eddy mode (identified with wavenumber $\lambda = p\mu$ and coefficient B) and comparatively little energy remains in the original mean mode (identified with wavenumber μ and coefficient A); the crosses in figure 5, and the data of figure 3, show this ratio to be about 4:1. Thus the steady-eddy flow resembles the initial laminar flow in character, but with B replacing A, the scale increased to the wavenumber $p\mu$ and the axes interchanged. Further, it is found that whenever $R > 2\frac{1}{2}$ the final value of B/ν likewise exceeds the critical value ($2\frac{1}{2}$) at which instability would occur in laminar flow, which suggests that the steady-eddy flow may itself be unstable (to still larger scales not yet allowed for in the calculations), and that it may break down in a similar way to the original laminar flow. If this is so then energy will appear at the even-smaller wavenumber $p^2\mu$.

But the steady state of the secondary eddy might similarly be unstable (generating energy at wavenumber $p^3\mu$) and so on in a cascade of instabilities, each taking energy to successively larger space scales. The kind of energy spectrum resulting from such a process is illustrated by the dots in figure 5, where the peaks, spaced a factor p^{-1} apart in wavelength, are apparent. The peaks are to be imagined to continue indefinitely to the left of $k = 1$, the energy-input wavelength. To the right, the spectrum will tail off roughly as indicated.

The data plotted here are obtained from the closure proposition that the eddies representing the breakdown of the mean flow are themselves subject to the action of eddies, *and* that these second-order eddies bear the same relation to the first-order eddies as the first-order eddies do to the mean flow.

Suppose that, in the fully cascaded turbulence, there results a functional relation between the forcing χ and the mean flow A. Dimensional considerations show that this can be written as

$$\chi = \nu^2\mu^3 f(A/\nu), \tag{7}$$

where the function f, representing the combined effect of the momentum transfer by the turbulence and by viscosity, is to be found. Consider the three-parameter approximation to the flow; the equations corresponding to A_1 and A_3 remain, as before,

$$\nu\mu^4 A + \tfrac{1}{2}\lambda\mu^3 BD = \mu\chi = \nu^2\mu^4 f(A/\nu), \tag{8}$$

$$\nu(\lambda^2+\mu^2)^2 D - \lambda\mu(\mu^2-\lambda^2)AB = 0. \tag{9}$$

However, for scale B there is the energy input forced from other modes, represented by the term $\frac{1}{2}\lambda^3\mu AD$, and the effect of the viscosity and the eddies generated by the B mode itself, which, according to the closure hypothesis, is represented by a term $\nu^2\lambda^4 f(B/\nu)$, where f is the same function as that defined by (7). Thus the set is closed by an equation analogous to (8), above, but involving B in place of A:

$$\tfrac{1}{2}\lambda^3\mu AD = \nu^2\lambda^4 f(B/\nu). \tag{10}$$

This takes the place of the previous equation $A_2 = 0$.

The system (8)–(10), together with the refined selection principle of §7 (entering figure 1 with argument $R_m = A/\nu$ in order to find λ), determines corresponding values of A, B, D and f; and figure 2 shows by the curve $3PC$ the relation between A and R, i.e. displays the inverse of the function f, for this three-parameter *cascaded* system.

Including the additional parameter E, but supposing the cascade still to operate only through the B scale, gives the four-parameter cascade system shown by the curve $4PC$.

Figure 2 shows that the intensity of the mean cascade flow lies between that of the laminar and steady-eddy solutions. This is not an unexpected result bearing in mind the weakening of the first-order eddy flow due to the action of the higher order eddies. The three-parameter and four-parameter approximations are in fair quantitative agreement over the range $2 < \chi/\nu^2\mu^3 < 9$, where the expression

$$\chi = 0{\cdot}62\mu^3 A^2 \quad \text{or} \quad f(A/\nu) = 0{\cdot}62\,(A/\nu)^2, \tag{11}$$

shown as the dashed curve in figure 2, is a close approximation. Remarkably, this is precisely the form in which the explicit effect of viscosity disappears, in the terms on the right-hand sides of (8) and (10), which represent the transfer of momentum by the eddies and by viscosity. Thus even for the modest values of the Reynolds number considered here the transfer of momentum by the turbulence is, within the likely error due to truncation, independent of the Reynolds number and is therefore likely to be that appropriate to the inviscid system. This is despite the fact that the energy *spectrum* is well within the viscous dissipation regime (see §9).

The four-parameter solution for all the coefficients is shown in figure 4, from which it can be seen that the dominance of the secondary flow over the primary is less marked when the energy cascades, compared with the situation when the

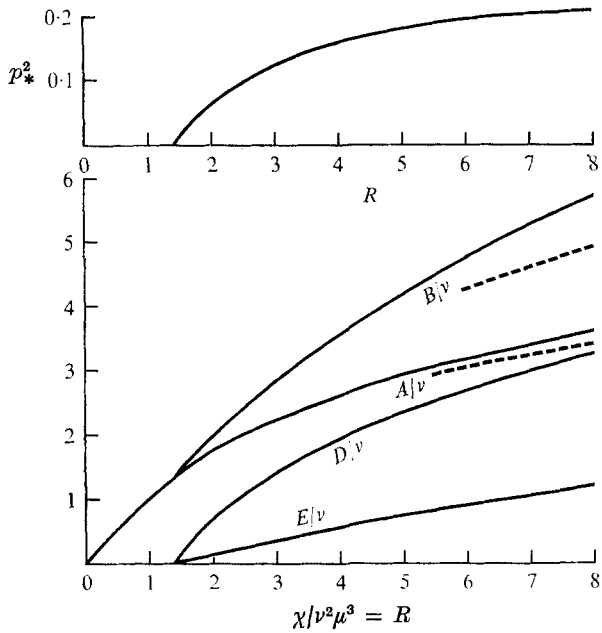

FIGURE 4. Dominant wavenumber p_* and flow coefficients as a function of the external forcing for the four-parameter approximation to cascade turbulence; the dominant wavenumber is that for the final mean flow. Dashed lines are A and B according to the three-parameter approximation, showing fair agreement over this range. Notice that the dominance of the first eddy mode B over the mean flow A is not now so marked as it was in, say, figure 3.

dissipation is viscous. This means that our assumption that the stability of the primary eddy could be considered independently of the mean flow is less obviously acceptable when the flow is cascaded. Though this throws some doubt on the notion of a cascaded system, at least in the simple form suggested here, the law for the spatial transfer of momentum by the eddies is unlikely to be modified substantially by the adoption of any other hypothesis for the transfer of energy to larger wavenumbers. For example, viscous dissipation of the eddy motion (e.g. the line $6P$ in figure 2) gives a stress law similar to that of (11) but with a numerical coefficient of about 1·4.

Again a numerical experiment could be designed to clarify the life history of flow consisting initially of two superposed harmonic modes. Also, because the penetration of energy to longer wavelengths occurs through the cascade mechanism a comparison between the spectrum resulting from a numerical model of two-dimensional turbulence and figure 5 would be valuable.

9. Energy spectrum

The data of figure 4 allow the spectrum of kinetic energy to be calculated for the truncated but cascaded system. For a given value of $\chi/\nu^2\mu^3$ values of A, B, D and E may be read off, the effect of the second-order cascade of energy starting with coefficient B being allowed for by (10). The values of the second-order

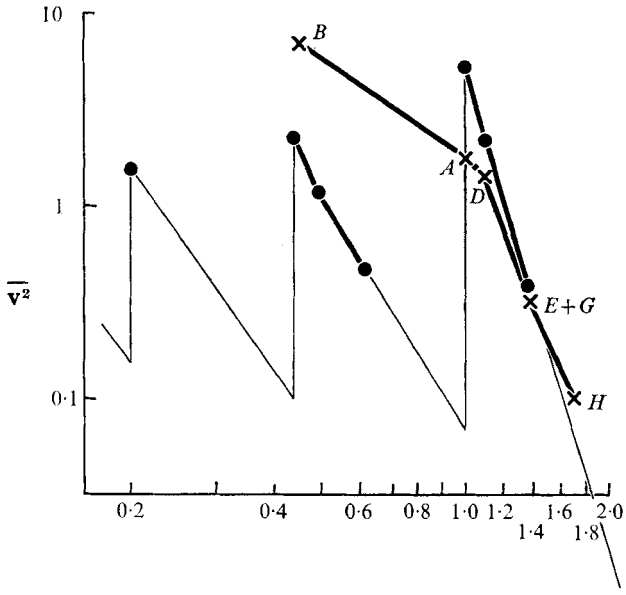

FIGURE 5. Example of the distribution of kinetic energy with wavenumber for flow with $R = \chi/\nu^2\mu^3 = 6$, plotted on logarithmic scales: ×, when the eddies are steady and controlled by viscosity; ●, when there is a cascade of eddies. The total wavenumber k, defined such that k^2 is the sum of the square of the wavenumbers in the x and y directions, is normalized so that $k = 1$ represents the scale of energy input. The spectrum is, of course, discrete and the lines joining the points are intended only to guide the eye. The steady-eddy solution is for the six-parameter system though the parameter G contributes so little energy that it is masked by that for E, which occurs at the same wavelength. The cascade solution is for the four-parameter system. Because only four parameters are available the shorter wavelength components of each mode are absent. Their likely behaviour is indicated by the thin lines.

coefficients can then be found by using the forcing to the second-order cascade: $\frac{1}{2}\lambda^3 AD$ in place of χ together with appropriate values of p from figure 1 using B/ν (in place of A/ν) for the value of R in the figure. By repeating this process the complete cascaded spectrum can, in principle, be calculated though we soon run out of the range of plausibility of figure 4 because the effective values of R increase at each stage. Thus the value $\chi/\nu^2\mu^3 = 6$ gives $A = 3{\cdot}15\nu$ for the mean flow (plotted at $k = 1$ in figure 5) and gives $B = 4{\cdot}75\nu$ for the first eddy mode (plotted at $k = 0{\cdot}45$), giving, somewhat uncertainly, $B = 8{\cdot}7\nu$ for the first cascade (plotted at $k = 0{\cdot}20$).

Enough data remain to show the general form of the spectrum. Comparing the cascade spectrum (dots in figure 5) with the viscous steady-eddy flow (crosses in figure 5), we notice that the penetration of energy into wavenumbers higher than that of the energy input (defined by $k = 1$ in figure 5) is nearly independent of the mechanism operating at lower wavenumbers. In fact the energy falls off like k^{-5} on the short-wave side: much faster than for an inertial subrange because we are still well inside the viscous dissipation range, even for the value

$$\chi/\nu^2\mu^3 = 12,$$

which is about the largest for which the calculations may be supposed reasonably accurate. At this value, 35 % of the dissipation of kinetic energy still takes place through the mean mode A (29 % through B and the cascade, 23 % through D and 13 % through E).

The spectrum at wavenumbers lower than the input wavenumber is very different in the two cases. With steady viscous control, long-wave energy appears at a single wavelength given by $k = 0{\cdot}45$, whereas in the cascaded system this mode splits into one longer component appearing at $k = 0{\cdot}20$ and a sequence of shorter modes extending off to the right. The longer mode splits similarly, giving rise to an indefinitely continued saw-tooth spectrum. According to figure 5 the kinetic energy falls off roughly in proportion to k on the long-wavelength side, and it is this comparatively great extension of energy into long waves that could be a decisive test of the theory.

I would like to record my thanks to Professor P. A. Sheppard, who, many years ago, stimulated my interest in the problem of the spectral distribution of energy emanating from a well-defined scale of input.

Appendix. Two-dimensional vorticity equation in wavenumber space

$$\nu\nabla^4\psi - \frac{D\zeta}{Dt} - \frac{1}{\rho}\frac{\partial F_x}{\partial y} = A_1 \sin\mu y + A_2 \cos\lambda x + A_3 \sin\lambda x \cos\mu y$$
$$+ A_4 \sin\mu y \cos 2\lambda x + A_5 \cos 3\lambda x + A_6 \sin 3\lambda x \cos\mu y + A_7 \cos\lambda x \cos 2\mu y + \ldots,$$

where

$$A_1 = \mu^2 dA/dt + \nu\mu^4 A + \tfrac{1}{2}\lambda\mu^3 BD + \tfrac{3}{2}\lambda\mu^3 GH - \mu\chi,$$

$$A_2 = \lambda^2 dB/dt + \nu\lambda^4 B - \tfrac{1}{2}\lambda^3\mu AD - \tfrac{3}{4}\lambda^3\mu DE - \tfrac{5}{4}\lambda^3\mu HE,$$

$$A_3 = (\lambda^2+\mu^2)\, dD/dt + \nu(\lambda^2+\mu^2)^2 D - \lambda\mu(\mu^2-\lambda^2) AB + \tfrac{1}{2}\lambda\mu(\mu^2+3\lambda^2) BE$$
$$- \tfrac{3}{2}\lambda\mu(\mu^2-5\lambda^2) GE,$$

$$A_4 = (\mu^2+4\lambda^2)\, dE/dt + \nu(\mu^2+4\lambda^2)^2 E - \tfrac{1}{2}\lambda\mu^3 BD + \tfrac{3}{2}\lambda\mu(\mu^2-8\lambda^2) DG$$
$$+ \tfrac{1}{2}\lambda\mu(\mu^2+8\lambda^2) BH,$$

$$A_5 = 9\lambda^2\, dG/dt + \nu 81\lambda^4 G + \tfrac{9}{4}\lambda\mu^3 DE - \tfrac{27}{2}\lambda\mu^3 AH,$$

$$A_6 = (\mu^2+9\lambda^2)\, dH/dt + \nu(\mu^2+9\lambda^2)^2 H - 3\lambda\mu(\mu^2-9\lambda^2) AG - \tfrac{1}{2}\lambda\mu(\mu^2+3\lambda^2) BE,$$

$$A_7 = -\tfrac{1}{2}\lambda^3\mu AD.$$

$$(\psi = A \sin\mu y + B\cos\lambda x + D \sin\lambda x \cos\mu y + E \cos 2\lambda x \sin\mu y + G \cos 3\mu y$$
$$+ H \cos\lambda x \sin 3\mu y.)$$

REFERENCES

FJØRTOFT, R. 1953 On the changes in the spectral distribution of kinetic energy for two-dimensional nondivergent flow. *Tellus*, **5**, 225–230.

GREEN, J. S. A. 1970 Transfer properties of the large-scale eddies and the general circulation of the atmosphere. *Quart. J. Roy. Met. Soc.* **96**, 157–185.

LIN, C. C. 1955 *The Theory of Hydrodynamic Stability*. Cambridge University Press.

LORENZ, E. N. 1963 Deterministic nonperiodic flow. *J. Atmos. Sci.* **20**, 130–141.

LORENZ, E. N. 1972*a* Barotropic instability of Rossby wave motion. *J. Atmos. Sci.* **29**, 257–264.

LORENZ, E. N. 1972*b* Low-order models representing realizations of turbulence. *J. Fluid Mech.* **55**, 545–563.